nuclear fusion
IAEA

PAPER • OPEN ACCESS

Interpretative TRANSP analysis of JET baseline scenario: performance dependence on plasma kinetic profiles

To cite this article: J. Lombardo *et al* 2025 *Nucl. Fusion* **65** 096009

OPEN ACCESS
IOP Publishing | International Atomic Energy Agency
Nuclear Fusion
Nucl. Fusion **65** (2025) 096009 (16pp)
https://doi.org/10.1088/1741-4326/adf4f6

Interpretative TRANSP analysis of JET baseline scenario: performance dependence on plasma kinetic profiles

J. Lombardo[1,2,*], F. Auriemma[1,3], V.K. Zotta[4], L. Garzotti[5], G. Pucella[6], M. Baruzzo[6], D. Frigione[1], Z. Ghani[5], D. Keeling[5], P. Lomas[5], S. Menmuir[5], F.G. Rimini[5], D. Van Eester[7], JET Contributors[a] and the EUROfusion Tokamak Exploitation Team[b]

[1] Consorzio RFX (CNR, ENEA, INFN, University of Padova, Acciaierie Venete SpA), C.so Stati Uniti 4, 35127 Padova, Italy
[2] CRF - University of Padova, Padova, Italy
[3] Istituto per la Scienza e la Tecnologia dei Plasmi, CNR, Padova, Italy
[4] Dipartimento di Ingegneria Astronautica, Elettrica ed Energetica, Sapienza University of Rome, via Eudossiana 18, Rome 00184, Italy
[5] United Kingdom Atomic Energy Authority, Culham Campus, Abingdon OX13 3DB, United Kingdom of Great Britain and Northern Ireland
[6] ENEA, Fusion and Nuclear Safety Department, C.R. Frascati, Via E. Fermi 45, 00044 Frascati, Italy
[7] Laboratory for Plasma Physics LPP-ERM/KMS, B-1000 Brussels, Belgium

E-mail: jacopo.lombardo@igi.cnr.it

Received 20 May 2025, revised 22 July 2025
Accepted for publication 28 July 2025
Published 8 August 2025

Abstract

The JET baseline scenario performances of the recent Deuterium–Tritium campaigns performed in 2021 (DTE2) and 2023 (DTE3) have been studied using the TRANSP code. This study focuses on the performance dependence on kinetic plasma parameters, emphasising the differences between the JET pulse #99512 from DTE2 and its counterpart JET pulse #104661 from DTE3. The auxiliary heating system in JET pulse #99512 did not operate at its full capacity, whereas in JET pulse #104661, it was possible to achieve additional 5.8 MW (∼25%). However, the expected enhancement in neutron production was not achieved. Detailed simulations reveal that the underperformance is due to a different combination of plasma dilution by impurities and main ion mixture compared to the conditions obtained in JET pulse #99512. The study demonstrates that a comprehensive modelling approach, integrating impurity effects and main ion composition, is essential to accurately reproduce the experimental neutron yield. The findings highlight the significant influence of spatial isotope distribution on neutron production, providing critical insights for optimizing performance in future fusion devices, including ITER.

[a] See Maggi *et al* 2024 (https://doi.org/10.1088/1741-4326/ad3e16) for JET Contributors.
[b] See Joffrin *et al* 2024 (https://doi.org/10.1088/1741-4326/ad2be4) for the EUROfusion Tokamak Exploitation Team.
[*] Author to whom any correspondence should be addressed.

Keywords: magnetic confinement, tokamak, JET, deuterium–tritium plasma, fusion performance, neutron rate, TRANSP

(Some figures may appear in colour only in the online journal)

1. Introduction

Research aimed at identifying a scenario capable of sustaining high fusion power, in anticipation of building increasingly more advanced experiments, is essential today. This research is made possible through intensive Deuterium–Tritium (DT) experimental campaigns on the JET tokamak device, where multiple scenarios are tested. Analysing the results makes it possible to determine which scenarios are the most efficient and high-performing.

The baseline scenario is one of the most extensively studied configurations to achieve sustained high fusion performance. This scenario features a high plasma current (I_p) and toroidal magnetic field (B_t), for reaching optimal confinement, characterized by high pedestal pressure and low collisionality. Furthermore, with the proper positioning of the divertor leg, a combination of edge-localized mode (ELM) pacing pellets and minimal gas injection can effectively reduce the density at the plasma separatrix, optimizing plasma performance in terms of energy confinement [1]. The work presented in this article focuses on the baseline scenario from the most recent DT campaigns at JET [2].

In the first JET DT experimental campaign in 1997 (DTE1) [3, 4], the first wall was made of carbon (C), and the maximum available power from the Neutral Beam Injector (NBI) was 24 MW, while the power from Ion Cyclotron Resonance Heating (ICRH) was 6-8 MW. This configuration demonstrated that stationary high-performance plasmas could be sustained, achieving 4 MW of fusion power for 5 s in a stationary type-I ELM H-mode plasma.

Before the start of the second DT campaign in 2020-21 (DTE2), significant upgrades were made: in 2011, to prevent the high retention and erosion rates of carbon, the wall was replaced with Beryllium (Be, $Z = 4$), and the divertor with Tungsten (W, $Z = 74$) [5]; the maximum NBI power was increased to ∼34 MW and the ICRH power to 6–8 MW. Given their significance in this work, among the various diagnostics, we specifically highlight the ^{235}U fission chamber detectors [6, 7]. In particular, these detectors are insensitive to neutron energy and capable of measuring neutron emission rates ranging from 10^{10} to over 10^{20} neutrons per second. The precise calibration of neutron detectors is crucial for accurately determining the time-dependent absolute fusion power produced in these plasmas. Owing to these advanced calibration procedures, which require detailed neutron transport calculations and dedicated plasma calibration discharges, the total uncertainty is below ∼10% [7–9].

As a result of these upgrades and the expertise gained and modelling efforts in preparation for the DTE2 campaign [10], it was possible to demonstrate a sustained high fusion power (P_{fus}) obtained in various scenarios, reaching the world record of P_{fus} over 10 MW for 5 s and generating 59 MJ of fusion energy in one plasma pulse [11]. This outstanding result was obtained in the so called non-thermal scenario, a variation of the hybrid scenario, designed to maximize the fusion rate of the beam-target (energetic ions hitting the thermal plasma ions).

Based on the lessons learned and the open issues from the DTE2 campaign, in 2023 the third DT JET campaign was conducted, named DTE3 [12, 13]. The goal of DTE3 was to support key physics and technological aspects for ITER and DEMO [14] and as a secondary goal to complete DTE2 experiments. One of the key differences between the two campaigns concerns the change in the neutral particles injected by the NBI: in the previous campaign a 50–50 DT mixture was injected, whereas in DTE3, only D neutrals were injected as suggested in [15], thus mimicking the ITER isotope choice for its NBIs.

In particular, this paper focuses on comparing and analysing the experimental data obtained from the baseline scenario at 3 MA of plasma current conducted during DTE2 and its continuation in DTE3. The goal is to understand the effects of the modifications made in DTE3 compared to the previous campaign, evaluating their impact on key plasma parameters, particularly the neutron rate (more sensitive to core performance), plasma stored energy, and confinement time.

1.1. Comparison of JET baseline scenario pulses: 99512 and 104661

To this aim, we specifically focused on the JET JET pulse #99512 from DTE2 and its counterpart in DTE3, JET pulse #104661. The latter is a closer engineering match of the DTE2 pulse with an increase in T gas puffing for compensating the pure D-NBI fuelling. Additionally, the total external heating power available is higher, as shown in figure 1. Both NBI and ICRH power have achieved an increase of approximately 4.5 MW and 1.3 MW, respectively, as reported in panels (*a*) and (*b*).

Both pulses are characterised by an ELMy (non-type I) H-mode scenario with beta normalised (β_N) values between 1.9 and 2. Plasma is affected by regular sawtooth occurrence in the core, with pellet-paced ELM frequencies in the 40 Hz range. The I_p is approximately 3.0 MA as reported in panel (*c*), and B_t between 2.8 and 2.9 T. The sub-divertor optical gas analyser (KT5P) [16] measured the isotope fractions, defined as the ratio between the Tritium density (n_T)

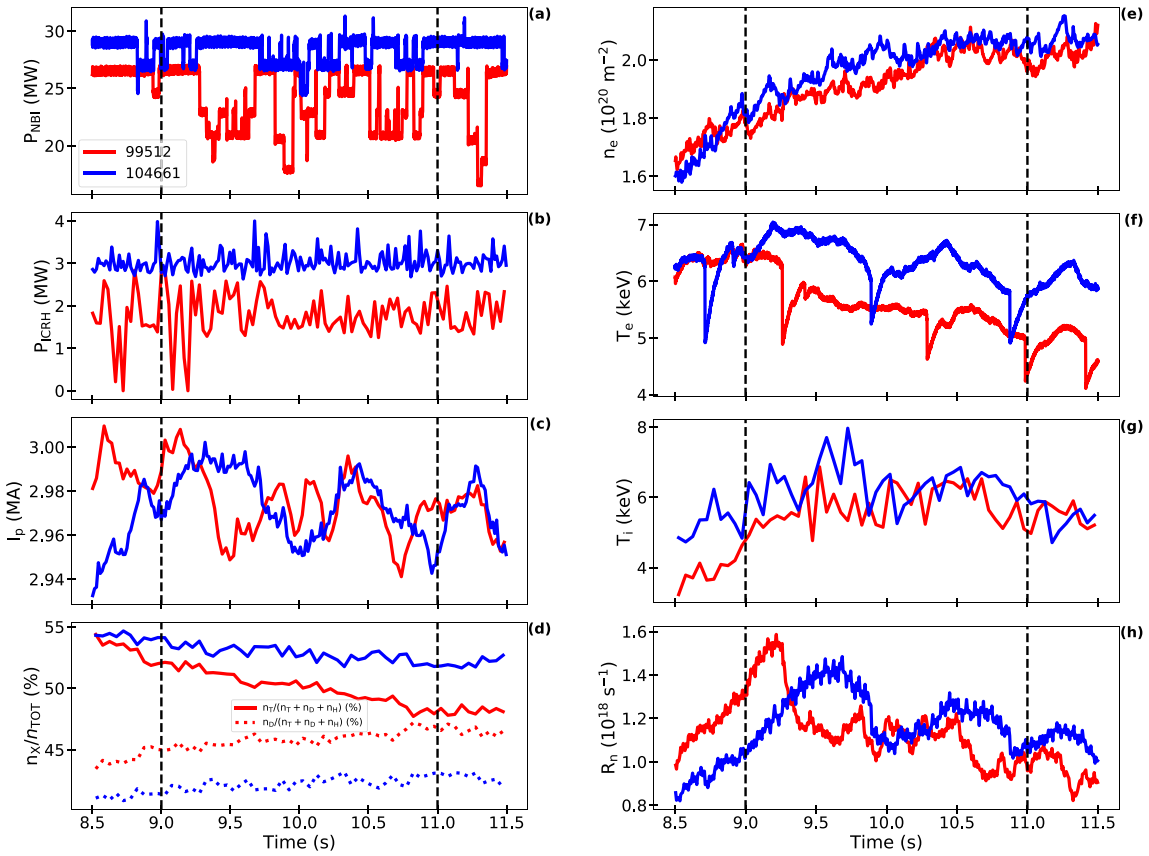

Figure 1. Comparison of the plasma main parameters time traces between DTE2 JET pulse #99512 (red line) and DTE3 JET pulse #104661 (blue line). The vertical black dashed lines delimit the time interval analysed in this paper—Panels (*a*): the power of Neutral Beam Injector (NBI); (*b*) the power of Ion Cyclotron Resonance Heating (ICRH); (*c*) the plasma current (I_p); (*d*) the isotope fractions of T in solid line, and D in dotted line; (*e*) the interferometric measurement of the line-integrated density passing through the central part of the plasma; (*f*) the electron temperature (T_e) measured by the fast ECE diagnostics; (*g*) the ion temperature (T_i), measured by CXRS diagnostics; (*h*) the neutron rate measured by fission chamber detectors.

or the Deuterium density (n_D) and the total hydrogenic species density (n_T+n_D+n_H). The pulses have a comparable isotope fraction (around 50D:50 T), as shown in panel (*d*). The electron density (n_e) in panel (*e*), measured by the interferometer, is similar in the two pulses. The ion temperature (T_i) in panel (*g*), measured by Charge-eXchange Recombination Spectroscopy (CXRS) diagnostics, is also comparable. An average 15% increase in the electron temperature (T_e) in panel (*f*), measured by fast Electron Cyclotron Emission (ECE) diagnostics, is observed in JET pulse #104461. This behaviour is consistent with expectations, as a greater amount of heating power is injected in this pulse. Moreover these two pulses feature similar magnetohydrodynamics (MHD), as reported in figure 2.

The higher external heating power in JET pulse #104661 (+4.5 MW from NBI and +1.3 MW from ICRH power compared to JET pulse #99512) is expected to enhance performance. On the other hand, a comparison of the experimental neutron rate shows similar measurements, as reported in panel (h), indicating that the DTE3 pulse is underperforming relative to expectations. The close comparison between the JET pulse #99512 and #104661 presented in this work will be focused on the time interval [9, 11] s, where the two discharges are in steady state condition.

1.2. Paper structure

This paper is structured as follows: section 2 describes the preparation of the input data required to run the simulations, with a particular focus on the fitting of the plasma kinetic profiles and equilibrium reconstruction. Section 3 presents the results of the TRANSP interpretative simulations for JET pulse #99512 (DTE2) and JET pulse #104661 (DTE3). While the simulation of JET pulse #99512 shows good agreement with experimental measurements, the simulation of JET pulse #104661 reveals a significant discrepancy between the neutron rate calculated by the code and the experimentally measured value. Section 4 analyses the potential causes of these differences and quantifies their relative contributions to the final result. To confirm the robustness of the approach, the same

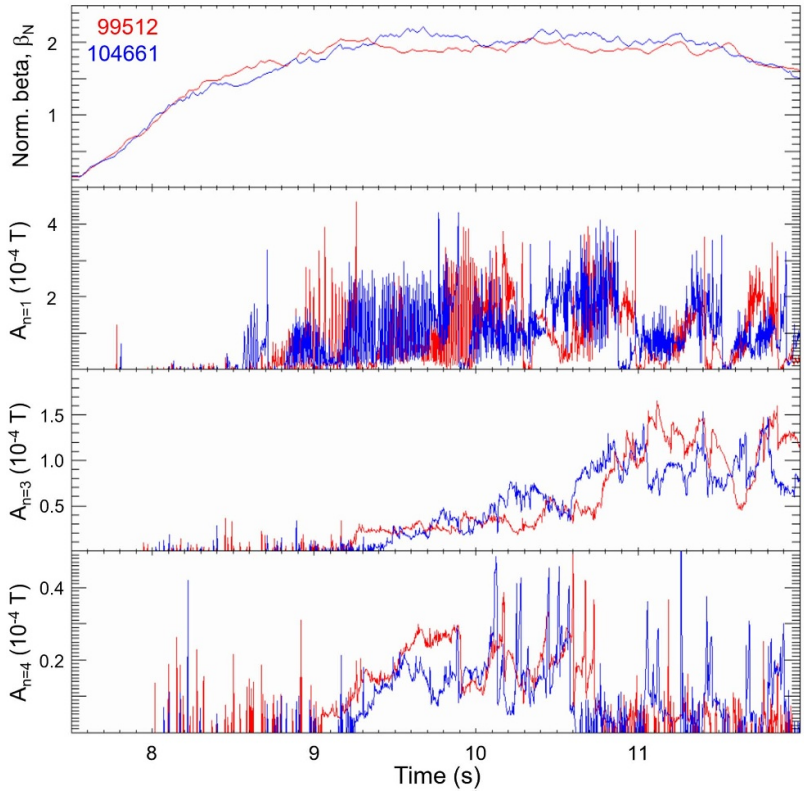

Figure 2. JET pulse #99512 (red lines) and JET pulse #104661 (blue lines). From top to bottom: normalised beta, amplitude of core $n = 1$ MHD activity (fishbones and continuous modes), amplitude of $n = 3$ tearing modes, amplitude of $n = 4$ tearing modes.

analysis was applied to JET pulse #104461, another DTE3 baseline pulse. Finally, sections 5 and 6 present the discussion of the impact of the equilibrium reconstruction on the outcome and conclusions, respectively.

2. Input data preparation and equilibrium reconstruction

The main numerical tool for the present analysis is the TRANSP code [17, 18]. The kinetic plasma profiles at each time step are provided as input to the code to perform high accurate interpretive analysis. The natural radial coordinate for TRANSP is the square root of the normalised toroidal flux ($\rho_{\rm tor}$), which reads 0 at the magnetic axis and 1 at the separatrix [19]. The main kinetic profiles electron density ($n_{\rm e}$); electron temperature ($T_{\rm e}$); ion temperature ($T_{\rm i}$); and plasma angular rotation (ω) are fit against the experimental data. The main diagnostics involved are the high-resolution Thomson scattering (HRTS) [20] for $n_{\rm e}$ and $T_{\rm e}$; the LIDAR [21] data for the $n_{\rm e}$ in the core region; the lithium beam emission spectroscopy (Li-BES) for the $n_{\rm e}$ in the edge region; and the CXRS diagnostics [22–24] for $T_{\rm i}$ and toroidal rotation ω in core and edge regions. In the simulations performed in this study, the equilibrium is fully prescribed in the TRANSP code. The EFIT++ [25] computes the equilibrium, considering the magnetic measurements and the total plasma pressure. To correctly calculate the total pressure profile, NUBEAM [26] computes the fast ion pressure in a preliminary TRANSP run on the same pulse. In NUBEAM, a fast ion is defined as an ion whose energy exceeds 1.5 times the thermal ion temperature. The experimental data are then mapped on the new equilibrium and fits are calculated, to be input in TRANSP, alongside the full equilibrium itself. This procedure can be iterated several times seeking convergence, although two iterations are usually sufficient to reconstruct a consistent equilibrium [27]. Figure 3(*a*) shows the comparison between JET pulse #99512 (red solid line) and JET pulse #104661 (blue solid line) in terms of the location of the flux surfaces obtained from the equilibrium reconstruction based on magnetic probe measurements, including the total plasma pressure (sum of the bulk thermal and fast particle pressures, as computed by TRANSP). It is crucial to correctly position the flux surfaces, taking into account the significant contribution of the fast ion pressure, in order to accurately fit the kinetic plasma profiles. Moreover, the equilibrium that includes the TRANSP pressure (EFTP) is compatible with a $T_{\rm e}$ at the separatrix ($T_{\rm e}(\rho = 1)$) of about 100 eV, whereas the misalignment in the separatrix location in the magnetic-only reconstruction provides a $T_{\rm e}(\rho = 1)$ in the range of 10–20 eV.

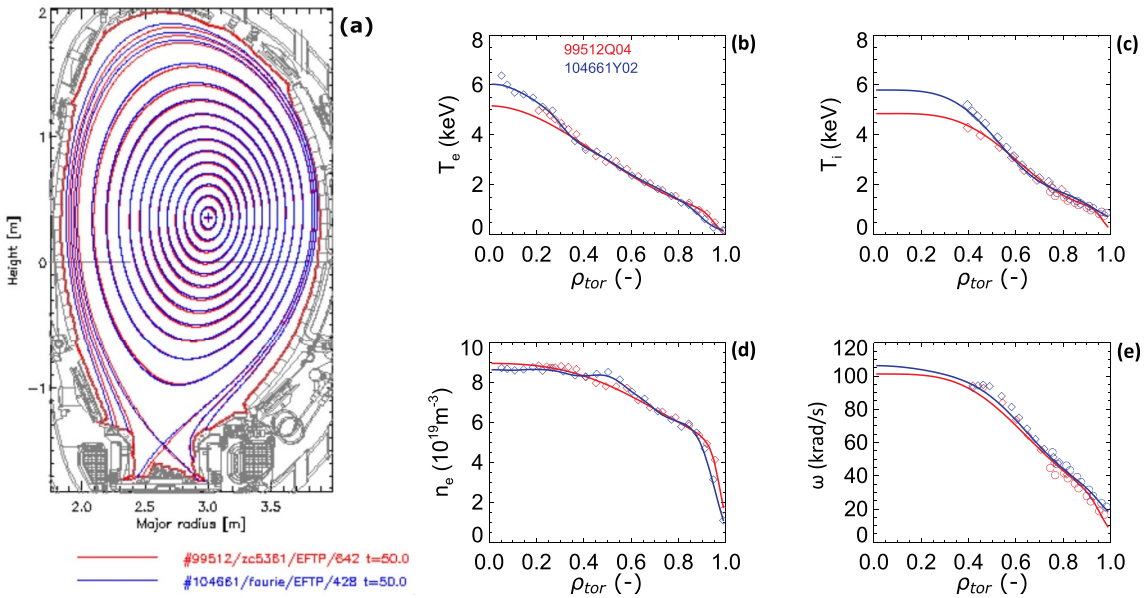

Figure 3. (*a*): he comparison between JET pulse #99512 (red) and JET pulse #104661 (blue) of the equilibrium reconstruction based on magnetic probe measurements, including the total TRANSP pressure (thermal + fast particles), at $t = 10.0$ *s*. In (*b*)–(*e*), the fits and measurements of the kinetic quantities are used as input for the TRANSP simulations. The fits are shown as solid lines, and the measurements are represented by empty symbols: red for JET pulse #99512 and blue for JET pulse #104661. The fits and the measurements are averaged over the time interval [9,11] s. (*b*): electron temperature (T_e); (*c*): ion temperature (T_i); (*d*): electron density (n_e); (*e*): plasma toroidal rotation (ω).

The fits are constructed using a combination of polynomial functions for the core region and hyperbolic tangent functions for the pedestal region. The figures 3(*b*)–(*e*) show the fits as solid lines and the measurements as empty symbols, of JET pulse #99512 in red and of JET pulse #104661 in blue. The fits and the measurements shown in the figure are averaged over the time interval [9,11] s. It is important to note that, in both cases, the n_e data are reduced to account for the cross-calibration between the HRTS diagnostics and the interferometer [27]. As mentioned, the DT plasma composition is based on measurements of KT5P located in the sub-divertor plenum. In the absence of additional information, the relative fraction of hydrogenic species measured in the sub-divertor is assumed to remain constant throughout the spatial profile of the plasma, considering the fast isotope mixing process [11, 28, 29].

3. TRANSP analysis

3.1. Interpretive TRANSP simulation of JET pulse #99512 from the DTE2 campaign

The analysis of the baseline pulse 99512 from the DTE2 campaign is performed using TRANSP in interpretive mode. The EFTP equilibrium is reconstructed using EFIT++ with the total plasma pressure from NUBEAM. For the data input preparation, the isotope mix is established around 50D:50 T, in agreement with the KT5P diagnostics.

The typical concentrations of the impurities used in the previous analysis on the JET experimental campaigns [30, 31] are as follows: Beryllium (Be, $Z = 4$) provides about 10^{-2} of the electron density, Nickel (Ni, $Z = 28$) around 10^{-4}, and Tungsten (W, $Z = 74$) around 10^{-5} as order of magnitude. Be, given its higher concentration and lower atomic number, is the species that primarily dilutes the plasma. Since the radiation is taken from measurements (and not self-consistently computed in the simulations) and considering the low dilution effect of W, the impurity mix used in the TRANSP simulations in this paper consists only of Be and Ni. In our simulations, the Be density is used as a proxy for all low-Z impurity density, while the Ni density serves as a proxy for all medium-Z impurities. The Be density (n_{Be}) is defined by prescribing a radially constant Be concentration ($c_{Be} = n_{Be}/n_e$). In the TRANSP simulations for JET pulse #99512, a value of $c_{Be} = 1\%$ was adopted, while the Ni concentration ($c_{Ni} = n_{Ni}/n_e$) $5 \cdot 10^{-4}$ is set, providing $Z_{eff} \sim 1.5$, being the value similar to that taken from the bremsstrahlung visible spectroscopy [32].

The results of each simulation are then compared with independent experimental quantities (e.g. plasma stored energy (W_{MHD}) [33], β_N, neutron rate, interferometer data, etc) to assess the quality of the run [27]. The total plasma stored energy in EFIT++ is defined as

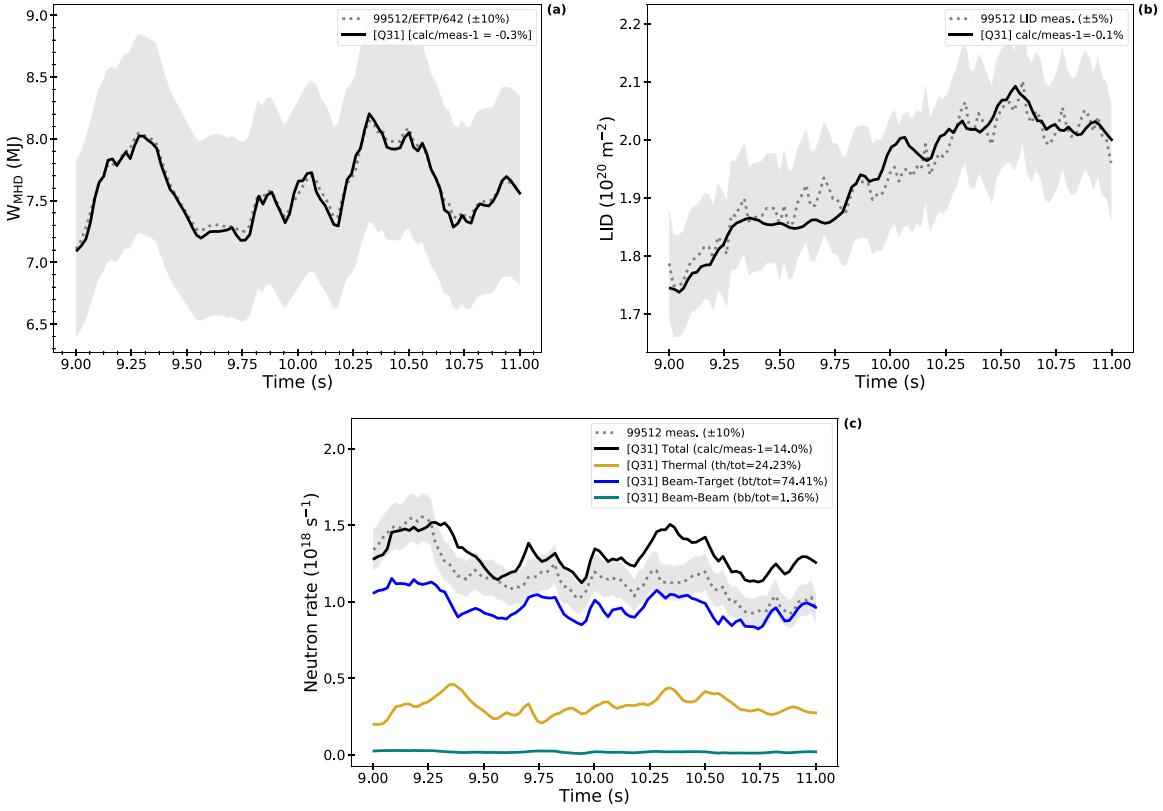

Figure 4. Comparisons, for the JET pulse #99512, between the experimental measurements (grey line with its confidence interval) and the TRANSP calculations (black line). (*a*): plasma stored energy (W_{MHD}); (*b*) displays the Line Integrated electron Density (LID) passing close to the magnetic axis; (*d*) Neutron rate measurement and the TRANSP calculation, whit the differentiation between the types of neutrons produced by various ion interactions (BT = blue line, TH = yellow line, BB = green line).

$$W_{\mathrm{MHD}}^{\mathrm{EFIT++}} = \frac{3}{2}\int p_{\mathrm{exp}}\mathrm{d}V \tag{1}$$

where p_{exp} is the fitted pressure profile obtained from the equilibrium reconstruction or, in our case, computed by TRANSP. From TRANSP, W_{MHD} can be computed as

$$W_{\mathrm{MHD}}^{\mathrm{TRANSP}} = W_{\mathrm{therm}} + \frac{3}{4}\left(W_{fi\perp} + 2W_{fi\parallel}\right) + 2W_{\psi} \tag{2}$$

where W_{therm}, $W_{\mathrm{fi}\perp}$, $W_{\mathrm{fi}\parallel}$ and W_{ψ}, represent the energy contributions from thermal pressure, fast-ion perpendicular pressure, fast-ion parallel pressure, and toroidal rotation, respectively [33]. Figure 4 reports the consistency checks for the simulation of this pulse, where the experimental measurements and EFIT++ calculation are shown as grey dotted lines and the quantities calculated by TRANSP as black solid lines. In figure 4(*a*), the W_{MHD} calculated by EFIT++ and the value calculated by TRANSP are in agreement within the confidence interval. The same pressure profile (computed by TRANSP) is used in both cases. Therefore, the minimal discrepancy between the two W_{MHD} values further confirms that the equilibrium iteration process has successfully converged. In figure 4(*b*), the comparison between the interferometric measurement of Line Integrated electron Density (LID), passing close to the magnetic axis, and the synthetic TRANSP LID calculations is shown. Due to the reduction applied to the n_{e} fit, the measurement and TRANSP calculation of LID are in good agreement, within a 5% confidence interval. In figure 4(*c*), the good agreement between the experimental and the TRANSP calculated neutron rate is shown, where the discrepancy results within the confidence interval of the experimental measurement. The trend of the TRANSP neutron rate result is in qualitative and quantitative good agreement with the time trace.

TRANSP allows the differentiation between the channels for fusion neutron production: thermal ion interactions (bulk-bulk, TH), fast-thermal ion interactions (beam-target, BT), and fast-fast ion interactions (beam-beam, BB). In the same figure 4(*c*), it can be seen that about one-quarter of the total neutrons come from TH reactions (yellow line), whereas the majority of neutrons (three-quarters) are produced by the BT reactions (blue line). The BB contribution accounts for less than 2% (green line).

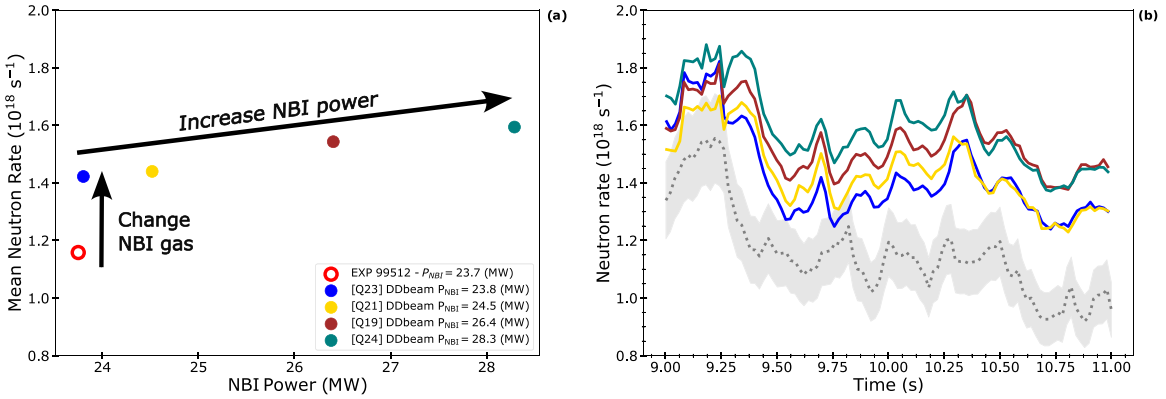

Figure 5. The TRANSP results after modifying the JET pulse #99512 simulations with only the DTE3 NBI configuration – (*a*): Average neutron rate versus the NBI power. The full dots represent the TRANSP simulation and the open dots represent the experimental values; (*b*) Neutron rate evolution in time for each extrapolation.

It is important to note that the DTE2 baseline pulses at 3.5 MA show a higher TH fraction, up to 50% of the total yield [27]. This means that, for the 3.0 MA pulse under analysis, the BT channel has a significant impact on the final neutron yield.

3.2. Extrapolation of JET pulse #99512 to DTE3 machine configuration

The comparison between the JET pulse #99512 simulation and the modified one to resemble the DTE3 NBI setup, provides information on the reliability and robustness of the modelling approach in describing the experimental behaviour of high-power baseline pulses.

Figure 5 shows the results of the TRANSP simulations done modifying the DTE2 setup toward the possible configurations available in the DTE3 campaign. The change of the NBI species and increase of the input power are separately introduced, in order to assess the relative weight of each modification. As shown in figure 5(*a*), changing the isotope composition of the NBI, from DT mix (50–50) to only D, without increasing the input power, would be expected to an increase in the neutron rate by about 25%. This behaviour is due to the more central deposition of the D beam, compared with the T beams and to the higher velocity of the D fast ions, which enables larger neutron production [15]. By increasing the NBI power from the quantity used in JET pulse #99512 (23.8 MW) to the power available in the DTE3 campaign (28.3 MW), the neutron rate increases linearly, becoming 40% larger than the JET pulse #99512 performances, as reported in figure 5(*b*). This result is in line with what is seen in the DTE2 experimental power scan [27].

It is important to note that the simulations extrapolated at the highest input power do not include any effects of the kinetic profiles, plasma composition, impurity levels, and ICRH power relative to the DTE3 baseline pulses. Only the increased fast ion population, due to the larger NBI power, is included. Therefore, we then expect that, by considering the correct input for the kinetic profiles, ICRH power, and other relevant parameters, the performance of the actual experimental plasma should be higher.

3.3. Interpretive TRANSP simulation of JET pulse #104661 from the DTE3 campaign

To ensure a fair comparison between JET pulse #99512 and its DTE3 counterpart, JET pulse #104661, a consistent preparation of input data and equilibrium reconstruction is essential to avoid any spurious effects introduced by differing procedures. In figure 3, the comparison of the averaged kinetic profile fits (n_e, T_e, T_i, and ω) between DTE2 JET pulse #99512 and DTE3 JET pulse #104661 has been already shown. The input profiles, obtained from the experimental fits of the two pulses examined, are comparable to each other. The JET pulse #104661 features a larger core T_e than JET pulse #99512, as a consequence of the increased input power. The T_e pedestal width of JET pulse #104661 turns out to be consistently larger than that of JET pulse #99512. Also, the n_e is slightly higher, while ω is comparable.

In JET pulse #104661, despite the good agreement between fitted profiles and experimental data a significant discrepancy in the neutron rate is reported in figure 6(*c*), with TRANSP overestimating the neutrons by 80%, while the other control parameters shown in figures 6(*a*) and (*b*), respectively W_{MHD} and LID are consistent with the experimental measurements.

The inconsistency between the calculation and the measured absolute value of the neutron rate indicates that one or more physical phenomena contributing to the performance reduction were not properly modelled. In particular, the overestimation of the neutron rate can be due to both thermonuclear and beam-target channels. This section aims to analyse the

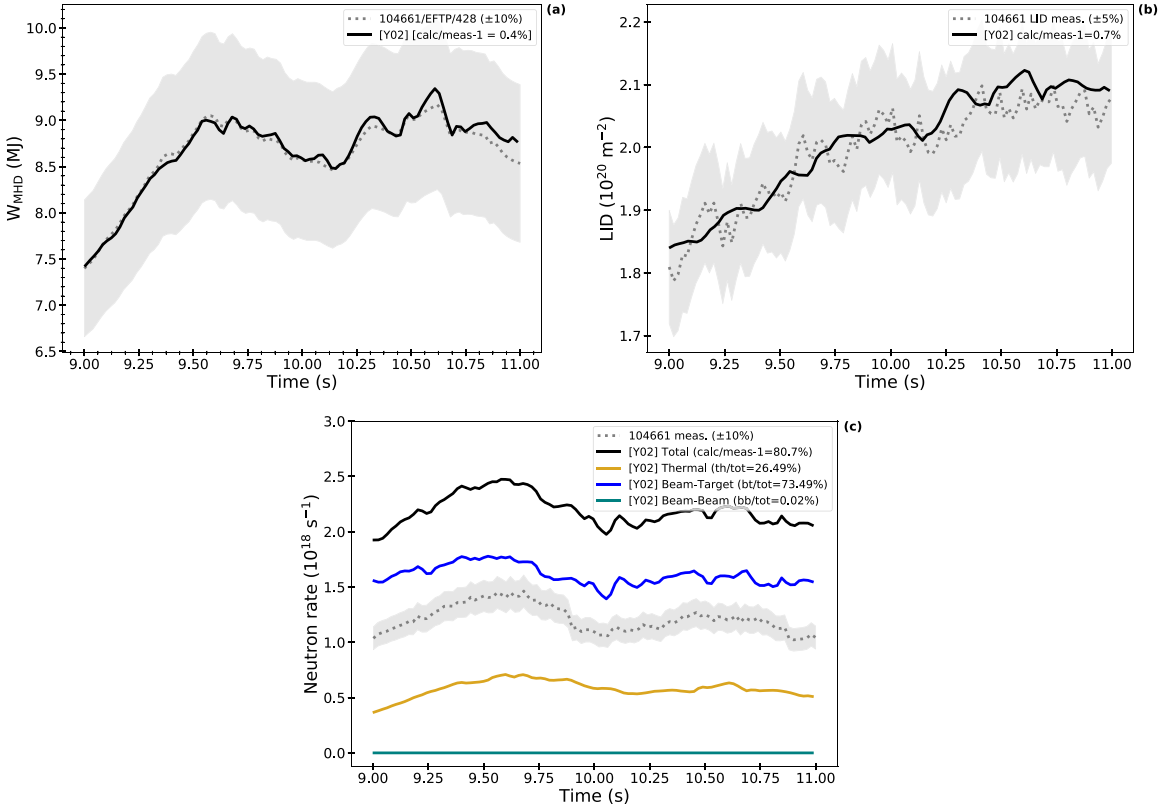

Figure 6. Comparisons, for the JET pulse #104661, between the experimental measurements (grey line with its confidence interval) and the TRANSP calculations (black line). (*a*): plasma stored energy (W_{MHD}); (*b*) displays the Line Integrated electron Density (LID) passing close to the magnetic axis; (*c*) neutron rate measurement and the TRANSP calculation, with the differentiation between the types of neutrons produced by various ion interactions (BT = blue line, TH = yellow line, BB = green line).

possible causes of such differences and quantify their relative contribution to the final result.

4. Key parameters influencing the fusion performance

In our TRANSP interpretative simulations, some input quantities are well-diagnosed (as the plasma equilibrium and the kinetic profiles), while others (impurities, hydrogenic isotope fractions) have greater uncertainty or rely on numerical computation (fast ion density). In particular, we aim to study the sensitivity of the TRANSP neutron calculation for the JET pulse #104661 to the dilution effect caused by impurities, as well as the impact of D beams on the core isotope mix. To study the effects of these changes on the neutron rate calculation, it was necessary to perform a scan for each parameter, introducing gradual changes starting from small perturbations up to significant variations in the result. Furthermore, this sensitivity study on key parameters, which are difficult to measure accurately, also helps to establish upper and lower limits where excessive variations in the parameter affect other independent measurements (e.g. a too large dilution will spoil the agreement with the W_{MHD} above the uncertainties on that quantity).

4.1. Dilution scan

The impurity mixes tested must be compatible with the experimental electron density and a plausible Z_{eff}. The reference effective charge value $\overline{Z_{\mathrm{eff}}}$ is taken from the bremsstrahlung visible spectroscopy, but since such diagnostic provides only indications due to calibration issues, a parametric scan of the Z_{eff} has been performed to overcome such limitation. To assess a wide range of Z_{eff}, a scan of $\pm 20\%$ and $\pm 10\%$ was performed around the reference value $\overline{Z_{\mathrm{eff}}} \sim 1.65$, taken from the measurement. Exploiting a simple model for plasma radiation [34], the experimental radiated power (10.4 MW) provides a possible estimate of the concentration of W and Ni. Assuming that W ($\langle Z_{\mathrm{W}} \rangle = 40$) accounts for approximately 90% of the total radiated power, while the remaining 10% is attributed to Ni ($\langle Z_{\mathrm{Ni}} \rangle = 28$) [35], it turns out that the c_{W} and c_{Ni} are respectively $6 \cdot 10^{-5}$ and $1.3 \cdot 10^{-4}$. Given these concentrations, the Z_{eff} contribution from mid and high Z impurities is $\Delta Z_{\mathrm{eff}}^{\mathrm{W,Ni}} = 0.2$. This implies that the contribution from low-Z impurities corresponds to the difference between the scanned Z_{eff} value and $\Delta Z_{\mathrm{eff}}^{\mathrm{W,Ni}}$. Assuming Be as a proxy for low-Z impurities in our simulations, each Z_{eff} value in the scan is associated with a specific Be concentration (c_{Be}). In this work, we focus on the sensitivity of plasma performance to dilution, which, as previously mentioned, is primarily driven by low-Z

Table 1. Range of the tested $Z_{\rm eff}$ values and corresponding Be concentrations ($c_{\rm Be}$).

$Z_{\rm eff}$	$c_{\rm Be}$ [%]
1.32	1.0
1.49	2.4
1.65	3.8
1.82	5.2
1.98	6.5

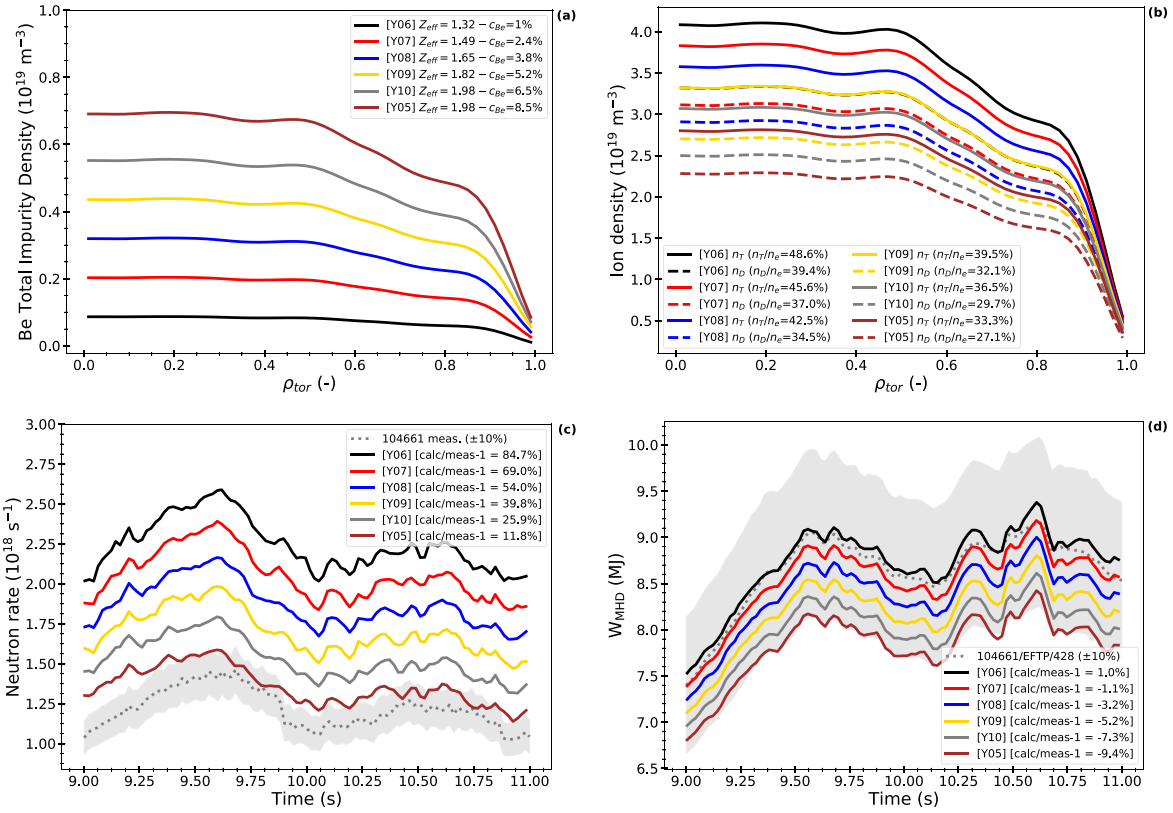

Figure 7. Effects of variations in Be concentration ($c_{\rm Be}$) = 1%, 2.4%, 3.8%, 5.2%, 6.5% and 8.5% for the JET pulse #104661. (*a*): time-averaged Be density profile, starting from the simulation, as in the reference case, with $c_{\rm Be}$ = 1% (black solid line) and then $c_{\rm Be}$ = 2.4%, 3.8%, 5.2%, 6.5% and 8.5%, respectively shown with red, blue, yellow, grey and brown solid lines. This colour scheme will be maintained throughout all figures; (*b*) the time averaged density profile between 9 and 11 s illustrates the variations in the T density ($n_{\rm T}$, solid line) and D density ($n_{\rm D}$, dashed line) profiles resulting from the dilution effect caused by the increased $c_{\rm Be}$; (*c*) shows the neutron rate time traces for these simulations comparison with the measurement (grey dotted line) with its confidence interval (±10%); (*d*) reports the $W_{\rm MHD}$ calculated from TRANSP (solid line) and the measurement (grey dotted line) with its confidence interval (±10%).

impurities. It is worth noting that evidence from physical testing of beryllium cladding erosion rates [36] supports the hypothesis of a possible level of beryllium contamination in the plasma.

The light impurity density directly affects the neutron rate calculation via the dilution of the bulk ions (D and T), reducing both the thermonuclear and the beam target channels. It also affects the beam penetration, but this effect is mild compared to the dilution. It is important to highlight that in our interpretive calculation with different impurity mixes, the self-consistently calculated radiated power does not affect the neutron rate because the electron temperature profile is set as input.

The analysed $Z_{\rm eff}$ values and their corresponding $c_{\rm Be}$ are reported in the table 1. In addition, a further test with $Z_{\rm eff}$ = 1.98 was carried out: in such run Be is imposed as being the only impurity present in the plasma. Although this assumption is not physically achievable, (e.g. the observed radiation power is not justified by only Be as impurity) it provides an estimate of the upper boundary for the dilution effect on neutron yield. Under this assumption, the level of $c_{\rm Be}$ becomes approximately 8.5%. Figure 7(*a*) shows the Be density profiles. The simulation with $c_{\rm Be}$ = 1%, as in the reference case, is shown by the solid black line. The others coloured solid lines (red, blue, yellow, grey and brown) represent the simulations with $c_{\rm Be}$ of 2.4%, 3.8%, 5.2%, 6.5% and 8.5%, respectively. This colour scheme is maintained throughout the figure. Figure 7(*b*) shows the variation in the $n_{\rm T}$ (solid line) and $n_{\rm D}$ (dashed line) profiles due to the dilution caused by the increased $c_{\rm Be}$. In the

most extreme dilution case (brown line), the D and T concentrations ($n_D/n_e, n_T/n_e$) are lowered by almost 15% for both ion species.

The reduction of n_D and n_T also leads to a reduction in the neutrons produced, as shown in figure 7(*c*). The average discrepancy between the measured and calculated neutron yield decreases from 80% in the reference simulation to 26% in the case of $c_{Be} = 6.5\%$. Agreement with the measurements can only be achieved in the case of maximum, albeit unlikely, dilution (c_{Be} ~8.5%). Further effects need to be investigated to explain the discrepancy between the experimental measurements and the simulations.

4.2. D and T density profiles assuming D core accumulation

In the interpretative simulations of JET pulse #104661, the D and T ion profiles are reconstructed based on the KT5P diagnostic assuming a fast isotope mixing process [11, 28, 29] which implies an isotope fraction constant along the radius. Such an assumption, despite the different particle fuelling channels for D (with beam + gas puffing) and T (with gas puffing only), leads to flat D and T concentration profiles.

The DTE3 experiments, with only a D source in the plasma core, can be prone to develop a different behaviour, with a radial shaped of the profile obtained from the ratio of the D and T profiles. To quantify such an effect, we used a model that, according to ion transport and sources, predicts the radial profiles of D and T. The JINTRAC [37] suite of codes, equipped with the first-principle based transport model QuaLiKiz [38], allows for predicting the deuterium density evolution, the tritium density evolution, the electron temperature and the ion temperature including the evolution of the impurity density profiles and the plasma current density. In this modelling framework the boundary conditions are imposed at the separatrix and the different fuelling channels for D and T can be modelled as gas puffing, pellets, and NBI injection. Predictive JINTRAC-QuaLiKiz simulations have been performed in order to obtain a first assessment of the particle sources and of the effect of transport on the main ion species in DTE3 [35]. However, the iteration between JINTRAC predictive and TRANSP interpretative simulations is needed to evaluate the effect of main ion concentration gradient on the actual experimental data. Previous work [39] has validated this modelling approach on JET baseline experiments, while the modelling of the different fuelling channels has been used for the design of the JET baseline fuelling scheme and for the verification of the model predictions on actual DTE2 data [40]. It is important to note that only the concentration is extracted from JINTRAC-QuaLiKiz to avoid any spurious effect due to the differences between the modelled profiles and the actual measurements. In those predictive simulations, the isotope ratio (D/T) at the edge is fixed according to residual gas measurements, whereas the internal radial profiles evolved according to the particle sources and transport. Since the total number of hydrogenic atoms is not changed, but only their relative magnitude, the W_{MHD} calculated by TRANSP is not affected by this modification and remains in agreement with the corresponding measurement within its confidence interval ($\pm$10%).

With JINTRAC-QuaLiKiz predictive runs, combined with the SANCO-ADAS [41, 42], it is also possible to predict the impurity concentrations of Be, Ni, and W. Simulations performed with TRANSP, where D, T, and impurities were taken from JINTRAC, were compared with simulations in which D and T were computed by JINTRAC and impurities were set as constant radial concentrations. The latter approach, although simpler, did not show significant discrepancies with the previous one in terms of dilution effect. This indicates that the assumption of flat concentrations of Be and Ni is consistent with the impurity transport calculations performed by JINTRAC. Therefore, in the subsequent analysis, we adopt this simplification.

Figure 8 compares the reference simulation and the simulation where the ion profiles are taken from the JINTRAC predictive run, represented by two solid lines in black and teal, respectively. Figure 8(*a*) shows the time averaged density profile of n_T (solid line) and n_D (dashed line), highlighting a flat tritium profile in the range [0, 0.5]. Figure 8(*b*) illustrates the isotope fractions' average in the same time range. The maximum variation in the n_T radial profile occurs in the range [0, 0.5], where its isotope fraction decreases from approximately 52% in the reference case to about 40% in the predicted case. At the edge, the predicted profiles match the KT5P measurements. A similar trend, but in the opposite direction, is observed for the n_D profiles. Figure 8(*c*) presents the neutron rate time traces for these simulations, compared with the measurement (grey dotted line) and its confidence interval ($\pm$10%). A 30% reduction in the discrepancy between the measurement and the TRANSP calculation is observed, leading to a calculated neutron rate that remains 50% higher than the measured value.

Using the JINTRAC predicted ion profiles, the most affected neutron yield channel is the BT, which shows a 20% decrease in the [0,0.4] ρ region. A marginal effect is also observed on the TH channel, with a 2% reduction compared to the reference simulation. The imbalance in the main ion mixture in the innermost regions, where neutron production is highest, has a significant impact on the neutron rate. The high NBI heating power combined with the high plasma density ensures that the primary neutron production mechanism is the BT reaction, while the BB contribution remains negligible, being 4 orders of magnitude lower than the BT term in these experiments.

Using only the isotope imbalance effect, a good agreement with the experimental neutron rate can be recovered only by assuming a non-realistic isotope fraction of approximately 30% T and 65% D.

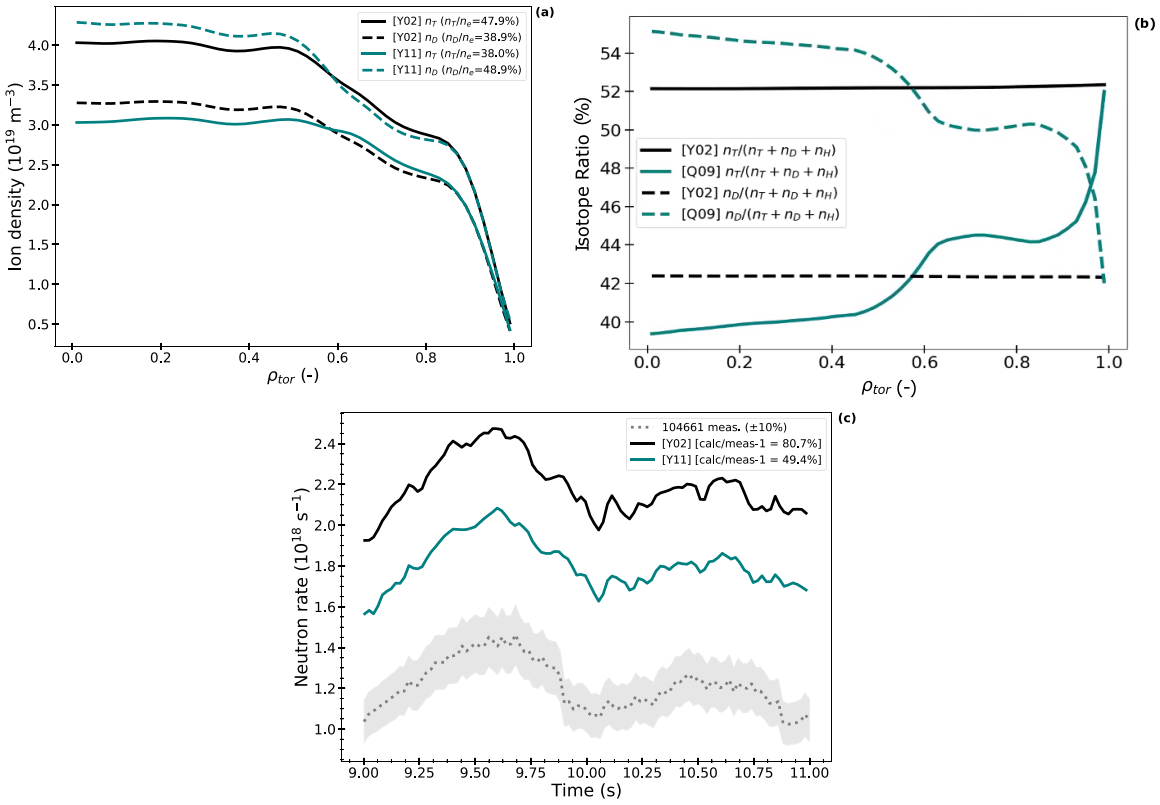

Figure 8. Comparison, for the JET pulse #104661, between the reference (black line) and the simulation with predicting the n_T and n_D radial profile (teal line). (*a*): Comparison between the time averaged n_T (with solid line) and n_D (with dashed line); (*b*): displays the isotope fractions average in the same time range; (*c*): shows the neutron rate time traces for these simulations comparison with the measurement (grey dotted line) with its confidence interval (±10%).

4.3. D accumulation effect combined with plasma dilution by impurities

In the two previous paragraphs, the dilution effect and the use of predicted ion profiles were analysed. For both cases, considered separately, their impact on the calculation of the neutron rate time profile is not sufficient to match the experimental data. In this paragraph, we combine those two effects. Neglecting the case with the maximum dilution $c_{Be} = 8.5\%$ (which is not realistic), we consider the cases with $c_{Be} = 1\%$, 2.4%, 3.8%, 5.2% and 6.5%, along with the predicted D and T ion profiles.

In figure 9, a comparison is shown between the cases of predicted n_D and n_T radial profiles with different levels of dilution. Five dilution levels are considered: $c_{Be} = 1\%$, as in paragraph 4.2 (teal lines), 2.4% (gold lines), 3.8% (pink lines), 5.2% (orange lines) and 6.5% (cyan lines). The plots compare the radial ion profiles (figure 9(*a*)) and the neutron rate evolution (figure 9(*b*)). The average value of n_T/n_e decreases from the reference value of 36% to 33% for $c_{Be} = 2.4\%$, 30% for $c_{Be} = 3.8\%$, 28% for $c_{Be} = 5.2\%$ and 25% for $c_{Be} = 6.5\%$. These significant reductions of core T concentration lead to a marked decrease in the neutron yield. The simulations using predicted ion profiles and the $c_{Be} = 3.8\%$ ($Z_{eff} = \overline{Z_{eff}}$), 5.2% ($Z_{eff} = \overline{Z_{eff}} \cdot 1.1$) and 6.5% ($Z_{eff} = \overline{Z_{eff}} \cdot 1.2$) result in neutron rate within the experimental confidence interval.

4.4. Interpretive TRANSP simulation of JET pulse #104461 from the DTE3 campaign

To further support the generality of the results obtained, a similar analysis was performed on JET pulse #104461, which is another counterpart of JET pulse #99512 within the DTE3 campaign. In this pulse at 9.8 s, a sawtooth crash occurs, leading to a temporary degradation of the performance until 10.2 s, when a recovery is observed. So the time interval between 9.8 and 10.2 s is excluded from the comparison between simulation results and experimental data for JET pulse #104461. In figure 10, a scan was performed to assess the effect of dilution (figure 10(*a*)), and the impact of using predicted ion profiles (teal line in figure 10(*b*)) was investigated. Four levels of dilution are tested: $c_{Be} = 1\%$ (black line), 3% (blue line), 5% (yellow line) and 6.5% (brown line), the latter corresponding to the case where beryllium is the only impurity present. As observed for JET pulse #104661, neither the inclusion of

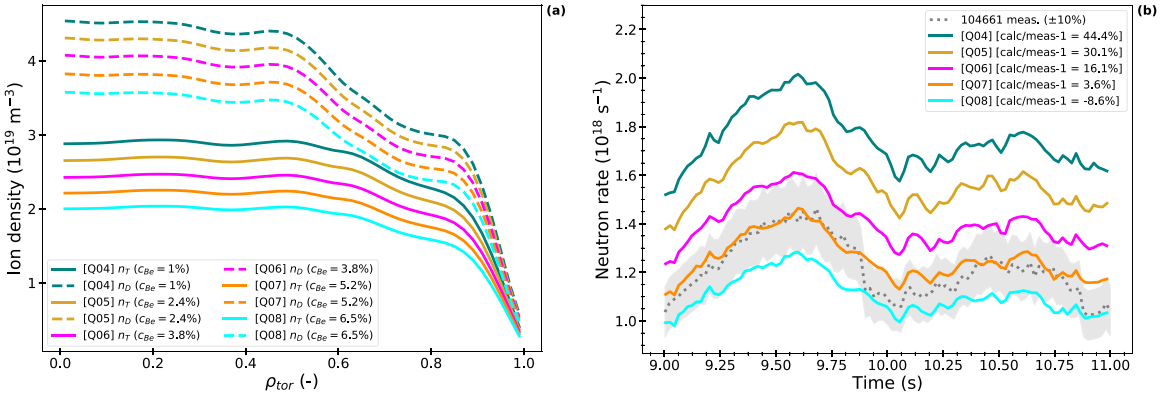

Figure 9. Comparison, for the JET pulse #104661, between the reference simulation and the simulations with predicted n_D and n_T radial profiles, considering five levels of dilution: $c_{Be} = 1\%$ (teal lines), 2.4% (gold lines), 3.8% (pink lines), 5.2% (orange lines) and 6.5% (cyan lines). (*a*): comparison of the density profiles for n_T (solid line) and n_D (dashed line); (*b*): neutron rate time traces for these simulations, compared with the experimental measurement (grey dotted line) and its confidence interval (±10%).

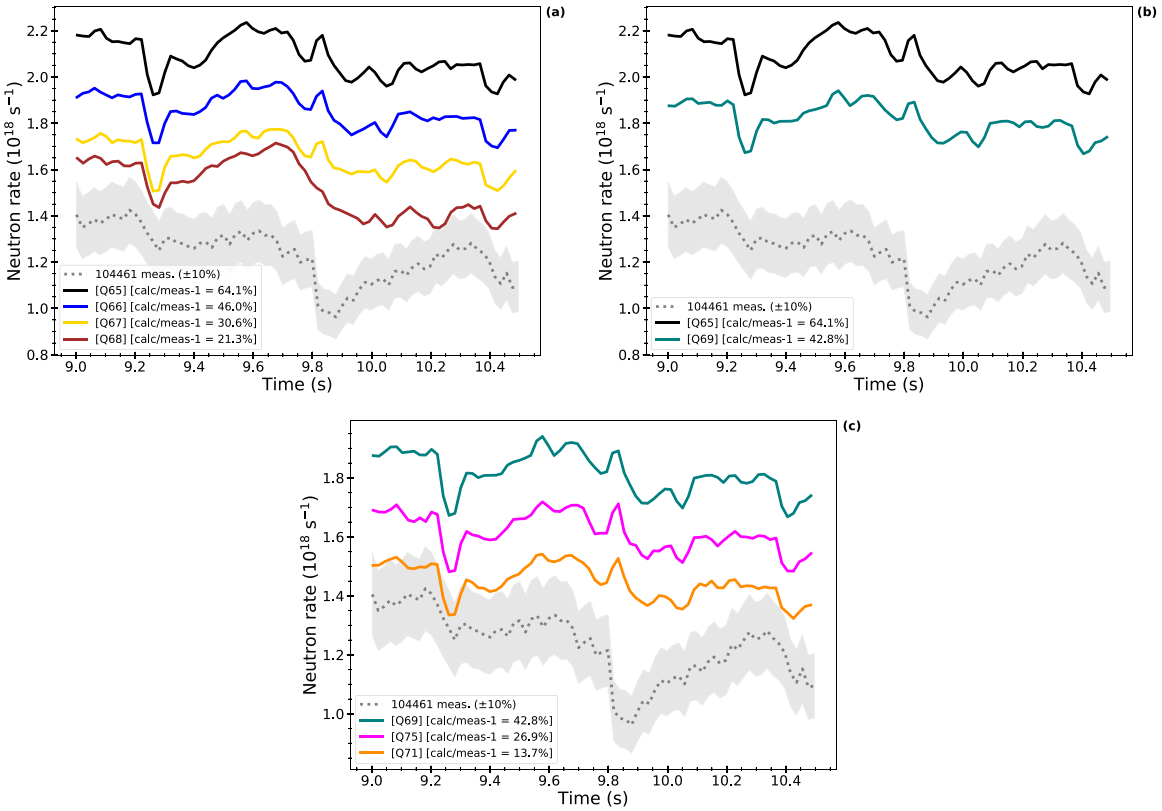

Figure 10. Impact on neutron rate prediction for JET pulse #104461 in the time window between 9.0 and 10.5 s, under different physical assumptions. (*a*) Effect of the dilution scan, where only the c_{Be} is varied (black line, 1%), (blu line, 3%), (yellow line, 5%) and (brown line, 6.5%); (*b*) effect of using predicted D and T radial profiles from JINTRAC (teal solid line) instead of flat 50%–50% profiles (black solid line); (*c*) Combined effect of dilution and predicted profiles considering three levels of dilution: $c_{Be} = 1\%$ (teal line), 3% (pink line), 5% (orange line), showing improved agreement with the experimental neutron rate within the confidence interval. The percentage values reported in the legend after the TRANSP labels are computed excluding the interval between 9.8 and 10.2 s.

dilution effects nor the use of predicted D-T profiles alone is sufficient to reproduce the experimentally measured neutron rate. In figure 10(*c*) both effects are combined, considering three levels of dilution: $c_{Be} = 1\%$ (teal line), 3% (pink line), 5% (orange line). The result of simulation with $c_{Be} = 5\%$ and predicted ion profiles is close to the experimental confidence interval, confirming the robustness of the approach across different baseline pulses in DTE3 campaign.

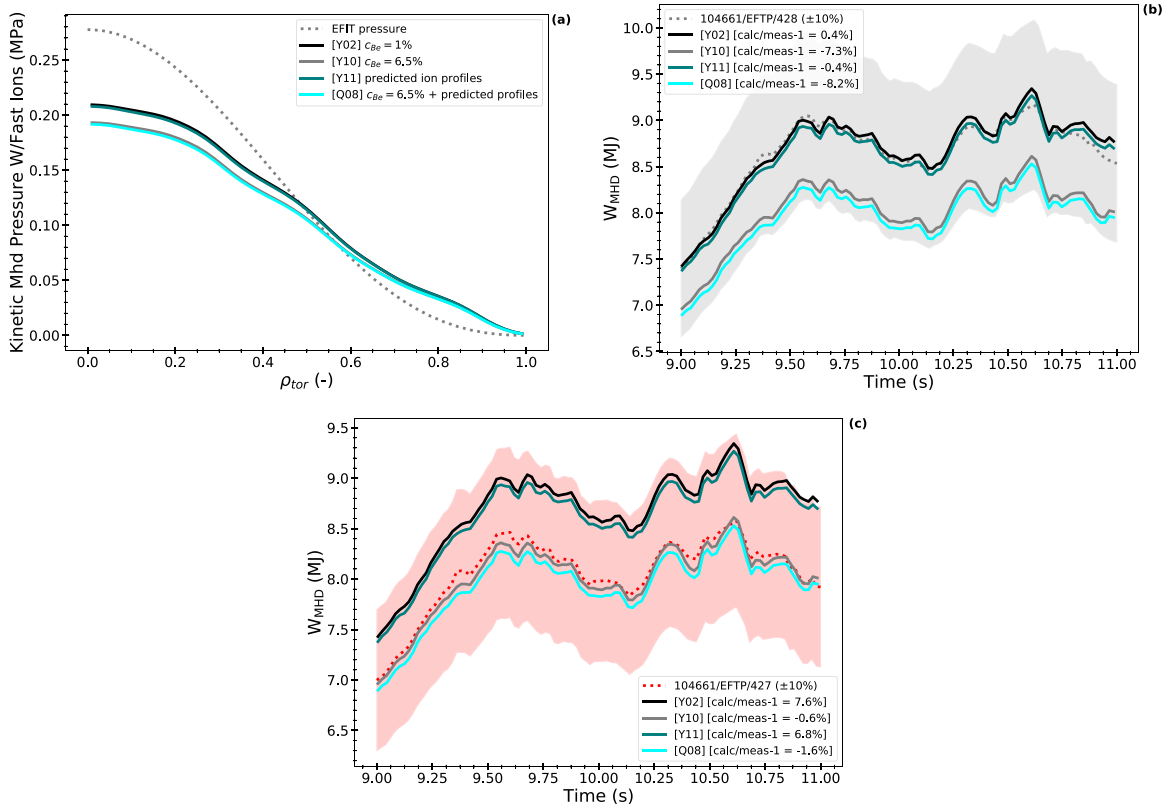

Figure 11. The influence of the tested effects (dilution and predicted ion profile) on the pressure profile for the JET pulse #104661 and on the plasma stored energy W_{MHD}. (*a*) also includes the initial pressure profile computed by EFIT; (*b*): the dotted grey line represents W_{MHD} calculated by EFIT using the equilibrium EFTP/428, reconstructed from the pressure profile of the reference simulation; (*c*): the dotted red line represents W_{MHD} calculated by EFIT using the equilibrium EFTP/427, reconstructed from the pressure profile of the simulation exhibiting the most altered pressure profile. The solid coloured lines represent the TRANSP simulations: reference (black line), the dilution case with $c_{Be} = 6.5\%$ (grey line), the case with predicted D and T radial profiles (teal line) and the combined effect of dilution and predicted ion profiles (cyan line).

5. Discussions on equilibrium consistency

In addition to the analyses presented in the previous sections, further investigations have been carried out to support and validate the results. In particular, special attention has been given to the equilibrium calculation, which is fundamental for profile mapping and all aspects related to plasma volumes. The sensitivity of the results to variations in the equilibrium reconstruction has been carefully assessed, verifying its impact on the consistency check quantities.

As reported in section 2, the EFTP equilibrium reconstructions used for the TRANSP simulation of JET pulse #99521 and 104661 are done including the total pressure (thermal + fast ion) from a preliminary TRANSP run. The preliminary TRANSP run is performed assuming $c_{Be} = 1\%$ and isotope fractions radially constant (reference, black line). However, in subsequent runs, modifications to the dilution altered the total pressure profile, as shown in figure 11(*a*). The figure shows how the simulations with $c_{Be} = 6.5\%$ (grey and cyan lines) result in a pressure reduction, particularly in the core. In contrast, the sole effect of the predicted ion profiles (teal line) does not alter the pressure profile. The same figure also includes the pressure profile calculated by EFIT at the first step (dashed grey line).

To ensure that these changes in the pressure profile do not introduce inconsistencies, it was verified that the equilibrium EFTP/428, produced using the pressure from the reference simulation (black line), remains consistent with the simulation exhibiting the most altered pressure profile (the simulation with predicted ion profiles and $c_{Be} = 6.5\%$, cyan lines). To verify this, starting from the simulation with the most altered pressure profile, an additional equilibrium was reconstructed with this pressure, the equilibrium EFTP/427. The comparison between the two equilibria, EFTP/427 and EFTP/428, shows that the difference in the position of the magnetic axes is within the reconstruction error (being lower than 1.5 cm). The largest effect appears to be on the elongation, which results slightly reduced in reconstruction with lower pressure. The variation of the elongation is, at its maximum, 5% which corresponds to an observed distance between two surfaces of 3–4 cm in the lower part of the machine.

Figures 11(*b*) and (*c*), reports the W_{MHD} values calculated by the EFIT++ for the two analysed equilibria. Figure 11(*b*) shows the equilibrium EFTP/428 (dotted grey lines) along with the corresponding TRANSP results, while figure 11(*c*) displays the equilibrium EFTP/427 (dotted red lines) compared with the same TRANSP outputs. In both cases, the values are shown along with their respective confidence intervals.

This demonstrates that the variability introduced by the modifications remains within the confidence interval of 10% for the W_{MHD} computed by EFIT++.

6. Conclusion

In this study, the TRANSP code was used for the interpretative analysis of the JET baseline scenario, focusing on JET pulse #99512 from the Deuterium-Tritium DTE2 campaign and JET pulse #104661 from the DTE3 campaign. Notably, in the latter campaign, the neutral particles injected by the NBI were exclusively D, whereas in DTE2, a 50-50 DT mixture was used. The results highlight that, in these two pulses, to enable a good agreement between the experimental neutron rate and the TRANSP modelled one, an accurate combination of dilution effects and core isotope mixing is needed.

In the analysis of JET pulse #99512, the identified combination includes a flat D and T concentration due to the fast ion mixture process [11, 28, 29] and c_{Be} of 1% which is the main dilution impurity.

Starting from the interpretative modelling of JET pulse #99512 we have substituted the DT NBI with pure D NBI and increased the power by 5 MW to simulate power achievable in the JET pulse #104661. The extrapolated neutron rate increased linearly and became 40% larger than the JET pulse #99512 performances, in line with what is seen in the DTE2 experimental power scan [27].

In the TRANSP simulations of JET pulse #104661, using the actual kinetic profiles obtained from the experimental data and the same combination as in JET pulse #99512 c_{Be} of 1% and a flat D and T concentration, a significant discrepancy of 80% emerged when comparing the TRANSP neutron rate calculation with the experimental one.

To study the mechanism underlying the disagreement between the predicted and actual performance of JET pulse #104661, proper tuning of dilution and core ion mixture has been performed. A scan of possible dilution levels was considered, alongside the effect of D core accumulation due to the D-NBI in the DTE3 campaign, in contrast with the D and T NBIs used in the DTE2 campaign.

It has been shown that the plasma dilution effect alone can explain the disagreement with the experimentally measured neutron rates only by assuming an unlikely level of c_{Be}, corresponding to the maximum Z_{eff} value in the scan and considering Be as the sole impurity. An effect of similar magnitude can be obtained when the consideration of D core density accumulation is included alone. Only combining the two effects it is possible to achieve agreement with the measurements in their confidence intervals.

The same analysis was also carried out for JET pulse #104461, leading to consistent results and thereby reinforcing the generality and robustness of the findings.

In this work, the relative importance of plasma dilution and core isotope mixture on the neutron yield was investigated. It turns out that proper tuning of these parameters is crucial to achieving a good match between the computed and experimental neutron rates. In particular, it is highlighted that, for this scenario, the assessment of the fusion yield in future machines relying on D-NBI core fuelling, such as ITER, must consider the source and transport effects on the ion relative fractions. Further analysis should clarify whether the combination of these effects could be expected in other DT scenarios developed at JET in its last campaigns. This will provide valuable insights for the design of the fuelling schemes in future DT devices.

Acknowledgments

This work has been carried out within the framework of the EUROfusion Consortium, funded by the European Union via the Euratom Research and Training Programme (Grant Agreement No 101052200 – EUROfusion) and from the EPSRC [Grant number EP/W006839/1]. Views and opinions expressed are however those of the author(s) only and do not necessarily reflect those of the European Union or the European Commission. Neither the European Union nor the European Commission can be held responsible for them.

Appendix. Anomalous fast ion diffusivity

The residual minor discrepancy observed between the simulations and the experimental neutron rate, despite the very good agreement in the consistency checks, may be attributed to several effects not accounted for in the simulations: uncertainties in nuclear cross-sections, models' approximations, and other unmodeled phenomena such as the MHD activity. To estimate the cumulative magnitude of these effects, we made a simple exercise ascribing (as a working hypothesis) the residual discrepancy to the fast ion population in the core a modulating it with an effective fast ion diffusion model. We report the anlaysis on the 104461 pulse, which has the largest residual discrepancy, but similar results have been obtained for other discharges presented in the paper. Indeed the thermal (TH) component of the neutron yield is directly linked to the bulk kinetic profiles, which are well diagnosed. In contrast, the beam-target (BT) neutron rate is the result of the NUBEAM calculation and can be influenced by numerous factors. The experimental NBI power, beam voltage, energy fractions, and their time evolution are consistently used as input in TRANSP. However, the BT neutron rate is highly sensitive to the fast ion density in the core, which is mainly affected by fast ion transport. TRANSP does not include a fully self-consistent model of fast ion transport, and a detailed analysis of fast ion losses is beyond the scope of this paper.

A simplified model can be incorporated into the simulations to estimate the magnitude of an effective, radially uniform fast ion diffusivity. Different levels of anomalous fast ion diffusivity (D_{fi}) can be included in the simulation to account for the fast particle losses and redistribution. Figure A1 shows a scan for three values of D_{fi}, taking as reference the simulation with

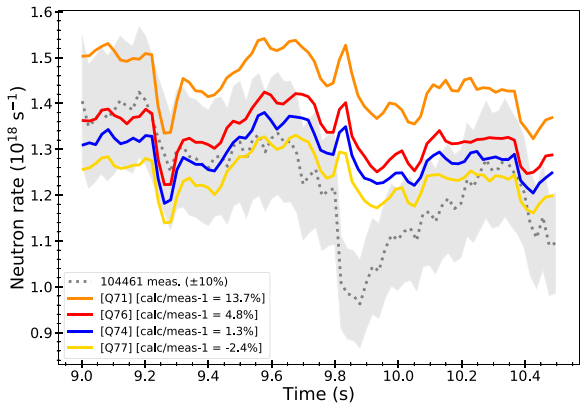

Figure A1. Starting from the case with a 5% dilution and predicted ion profiles (orange line) for the JET pulse #104461, a scan of the fast ion diffusivity (D_{fi}) is performed. Four diffusivity levels are considered: $D_{fi} = 0$, 0.5, 1, and 1.5 m^2 s^{-1}, represented by orange, red, blue, and yellow lines, respectively. The percentage values reported in the legend after the TRANSP labels are computed excluding the interval between 9.8 and 10.2 s.

the smallest discrepancy from the experiment, the $c_{Be} = 5\%$ and predicted ion profiles (orange line) in figure 10(*c*). The D_{fi} values analysed are 0.5, 1, and 1.5 m^2 s^{-1}, represented by red, blue, and yellow lines, respectively.

The presence of an anomalous fast ion diffusivity closes the gap between the modelled and the experimental neutron rate which turns out to be within 10% for all values of D_{fi}, confirming that such parameter lies between 0.5 and 1.5 m^2 s^{-1}. It is beyond the scope of this paper to finely determine the value of the parameter D_{fi}, but some considerations can still be made. The value of 1 m^2 s^{-1} provides the best agreement in the steady state phase (i.e. far from the sawteeth), whereas 1.5 m^2 s^{-1} provides a generally lower neutron rate and gives the smallest value of the ratio between modelled and experimental neutron rate.

ORCID iDs

J. Lombardo 0009-0007-9349-0246
F. Auriemma 0000-0002-1043-1563
V.K. Zotta 0000-0002-3518-5178
L. Garzotti 0000-0002-3796-9814
G. Pucella 0000-0002-9923-2770
M. Baruzzo 0009-0006-7853-7280
D. Keeling 0000-0002-3581-7788
F.G. Rimini 0009-0001-2917-0455
D. Van Eester 0000-0002-4284-3992

References

[1] Garzotti L. *et al* 2019 *Nucl. Fusion* **59** 076037
[2] Garzotti L. *et al* 2025 *Plasma Phys. Control. Fusion* **67** 075011
[3] Jacquinot J. *et al* 1999 *Nucl. Fusion* **39** 235
[4] Keilhacker M. *et al* 1999 *Nucl. Fusion* **39** 209
[5] Matthews G.F. *et al* 2007 *Phys. Scr.* **2007** 137
[6] Syme D.B. *et al* 2012 *Nucl. Eng. Des.* **246** 185–90
[7] Batistoni P. *et al* 2017 *Rev. Sci. Instrum.* **88** 103505
[8] Štancar Ž. *et al* (JET Contributors) 2019 *Nucl. Fusion* **59** 096020
[9] Čufar A. *et al* 2018 *Fusion Sci. Technol.* **74** 370–86
[10] Garcia J. *et al* (JET Contributors) 2023 *Nucl. Fusion* **63** 112003
[11] Maslov M. *et al* (JET Contributors) 2023 *Nucl. Fusion* **63** 112002
[12] Maggi C. *et al* 2024 *Nucl. Fusion* **64** 112012
[13] Joffrin E. *et al* 2024 *Nucl. Fusion* **64** 112019
[14] Kappatou A. *et al* 2025 *Plasma Phys. Control. Fusion* **67** 045039
[15] Van Eester D. *et al* (JET Contributors) 2022 *Plasma Phys. Control. Fusion* **64** 055014
[16] Vartanian S. *et al* 2021 *Fusion Eng. Des.* **170** 112511
[17] Hawryluk R. 1980 *Physics of Plasmas Close to Thermonuclear Conditions* vol 1 pp 19–46
[18] Breslau J., Gorelenkova M., Poli F., Sachdev J., Pankin A., Perumpilly G., Yuan X. and Glant L. 2018 TRANSP (https://doi.org/10.11578/dc.20180627.4) (Accessed June 2018)
[19] Pankin A.Y., Breslau J., Gorelenkova M., Andre R., Grierson B., Sachdev J., Goliyad M. and Perumpilly G. 2025 *Comput. Phys. Commun.* **312** 109611
[20] Frassinetti L., Beurskens M.N.A., Scannell R., Osborne T.H., Flanagan J., Kempenaars M., Maslov M., Pasqualotto R. and Walsh M. (JET-EFDA Contributors) 2012 *Rev. Sci. Instrum.* **83** 013506
[21] Maslov M., Beurskens M.N.A., Kempenaars M. and Flanagan J. 2013 *J. Instrum.* **8** C11009
[22] Thorman A., Litherland-Smith E., Menmuir S., Hawkes N., O'Mullane M., Delabie E., Lomanowski B., Fontdecaba J.M. and Scully S. (JET Contributors) 2021 *Phys. Scr.* **96** 125631
[23] Delabie E., Hawkes N., Biewer T.M. and O'Mullane M.G. (JET Contributors) 2016 *Rev. Sci. Instrum.* **87** 11E525
[24] Hawkes N.C., Delabie E., Menmuir S., Giroud C., Meigs A.G., Conway N.J., Biewer T.M. and Hillis D.L. (JET Contributors) 2018 *Rev. Sci. Instrum.* **89** 10D113
[25] Lao L., St John H., Stambaugh R., Kellman A. and Pfeiffer W. 1985 *Nucl. Fusion* **25** 1611
[26] Pankin A., McCune D., Andre R., Bateman G. and Kritz A. 2004 *Comput. Phys. Commun.* **159** 157–84
[27] Štancar I.Z. *et al* 2023 *Nucl. Fusion* **63** 126058
[28] Maslov M. and *et al* (JET Contributors) 2018 *Nucl. Fusion* **58** 076022
[29] Bourdelle C. *et al* (JET Contributors) 2018 *Nucl. Fusion* **58** 076028
[30] Telesca G. *et al* (JET Contributors) 2024 *Nucl. Fusion* **64** 066018
[31] Wendler N. and Pucella G 2024 *Nucl. Mater. Energy* **41** 101743
[32] Maggi C.F. *et al* (JET-EFDA Contributors) 2012 *Rev. Sci. Instrum.* **83** 10D517
[33] Giannone L. *et al* (JET Contributors) 2021 *Nucl. Fusion* **61** 066021
[34] Mazzotta C., Pucella G., Giovannozzi E., Marinucci M. and *et al* (FTU Team) 2022 *Nucl. Fusion* **62** 026004
[35] Zotta V.K. *et al* 2024 50th *EPS Conf. on Plasma Physics* (*Spain, 8–12 July 2024*) P1-040
[36] Dittrich L. *et al* 2021 *Phys. Scr.* **96** 124071
[37] Romanelli M. *et al* and (EFDA-JET Contributors) 2014 *Plasma and Fusion Research* **9** 3403023

[38] Bourdelle C. *et al* (JET Contributors) 2015 *Plasma Phys. Control. Fusion* **58** 014036
[39] Zotta V. *et al* (JET Contributors) 2022 *Nucl. Fusion* **62** 076024
[40] Zotta V.K. *et al* 2022 *48th EPS Conf. on Plasma Physics. P2a.115* (*27 June–1 July 2022*)
[41] Taroni L., Alper B., Giannella R., Marcus F., Smeulders P., Von Hellermann M., Lawson K. and Mattioli M. 1994 *Impurity Transport of High Performance Discharges in JE JET-P–94-29* pp 163–8
[42] Pütterich T., Fable E., Dux R., O'Mullane M., Neu R. and Siccinio M. 2019 *Nucl. Fusion* **59** 056013